Uncertainty quantification for random fields estimated from effective moduli of elasticity

Jack Pierce-Brown,[1*] Luis C. Neves,[1] and Donald L. Brown[2]

[1] *Faculty of Engineering, University of Nottingham, United Kingdom*
[2] *School of Mathematical Sciences, University of Nottingham, United Kingdom*
[*] Corresponding author: jack.piercebrown[at]nottingham.ac.uk

Abstract

The stochastic finite element method is a useful tool to calculate the response of systems subject to uncertain parameters and has been applied extensively to analyse structures composed of randomly heterogeneous materials. The methodology to estimate the parameters of the random field underlying a stochastic finite element model often utilises the midpoint approximation wherein material properties that are measured over a sample volume are treated as point observations of the random field at the centroid of the sample volume. This paper investigates the error induced by this approximation for the case of effective moduli of elasticity resulting from tensile loading as well as 3 and 4-point bending. A computer experiment has been performed consisting of the generation of synthetic stiffness profiles from a lognormal stochastic process, the calculation of effective properties as weighted harmonic averages and the estimation of random field parameters through the method of moments. The uncertainty in the parameter estimates is quantified and a recommendation is made as to which bending test is superior for obtaining random field parameter estimates with reference to the statistics of the base process and the tensile loading condition.

Keywords: Uncertainty Quantification, Effective Elastic Modulus, Midpoint Approximation, Random Field Theory, Stochastic Finite Element Method

1 Introduction

The stochastic finite element method is a useful tool to calculate the response of systems subject to uncertain parameters [1] and has been applied extensively to analyse structures composed of randomly heterogeneous materials such as timber [2], concrete [3] and soil [4]. The mathematical model for spatial variation of material properties that underlies stochastic finite element modelling is random field theory [5]. This paper considers the variation of modulus of elasticity E with spatial parameter v modelled by a random field $E(v)$ parametrised by a location parameter μ, scale parameter σ and a correlation parameter θ known as the *correlation length* [6]. The accuracy of the response distribution obtained by the stochastic finite element method depends on the uncertainty associated with the estimation of the parameters of the base random field. Conventional statistical methodologies to estimate the parameters of the random field model require point observations of the base random field $E(v)$ however experimentally determined material properties are in fact *effective* material properties E^* constituting an average over the sample volume. The effective property E^* of a heterogeneous material is the property of the homogeneous equivalent that produces identical behaviour with respect to some measurable quantity such as displacement in the case effective modulus of elasticity, flow in the case of effective hydraulic permeability and voltage in the case of effective conductivity [7].

The problem of the incompatibility between the inferential requirement for point observations of the underlying random field $E(v)$ and the reality that material properties can only be measured over a non-zero volume is often resolved through the use of the midpoint approximation [8]. This approximation treats the effective property E^* that is obtained over the sample volume as a point observation of the base process $E(v)$ at the centroid v_c of the sample volume. Figure 1 illustrates the error $\epsilon = E(v_c) - E^*$ that results from the midpoint approximation and it is argued that this approximation is responsible for significant uncertainty in the estimated parameters of the random field $E(v)$. This paper presents the results of a computer experiment that has been conducted to quantify parameter uncertainty by comparing the distribution of the parameter estimates obtained from the effective properties under the midpoint approximation to the distribution of statistics of the random field. The total uncertainty is composed of two sources [9] namely aleatoric uncertainty which is the statistical uncertainty due to limited sample size and epistemic uncertainty which is the systematic uncertainty due to estimator bias primarily resulting from the utilisation of the midpoint approximation.

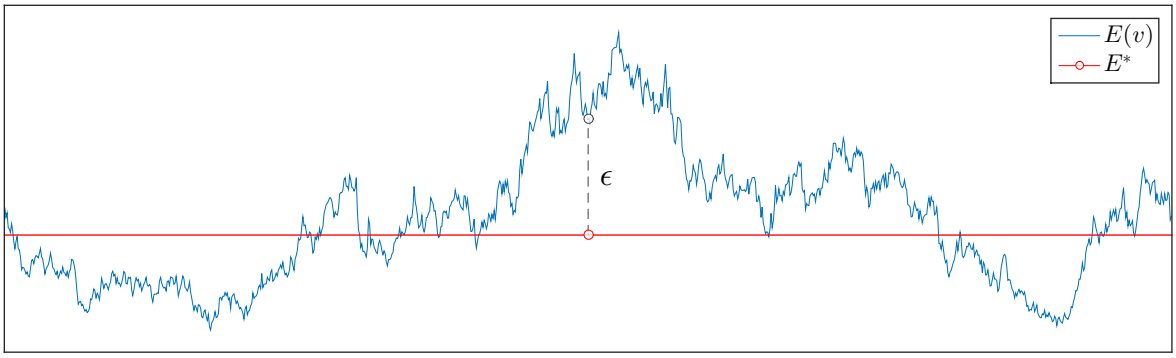

Figure 1: Midpoint approximation error ϵ between the base process $E(v)$ and effective property E^*.

The motivation for selecting modulus of elasticity E as the material property considered in this paper is due to the importance of this material property to the grading of timber which seeks to assign timber elements into strength classes for structural use. However the methodology and results contained within this paper are also applicable to other effective properties which are averages over the underlying random field. In particular this paper considers the effective elastic modulus E^* of a simply supported beam obtained by three different tests namely 3-point P_3 and 4-point P_4 bending resulting in midspan deflection U_B as well as tension loading P_T resulting in total displacement U_T as shown in Figure 2.

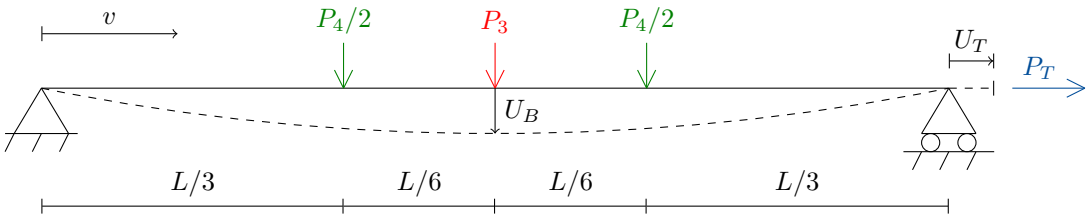

Figure 2: 1D model of a simply supported beam of length L under 3-point loading P_3, 4-point loading P_4 resulting in midspan deflection U_B as well as tensile loading P_T resulting in total deflection U_T.

This paper presents the formulation of the effective modulus of elasticity E^* of a Euler-Bernoulli beam as a weighted harmonic mean. This formulation offers a compelling alternative to the finite element method for obtaining the displacement of a heterogeneous beam at a single spatial location. The derivation for the case of the 4-point effective property E_4^* is shown in the Appendix otherwise for the case of the 3-point effective property E_3^* see Bechtel [10] or the case of tension E_T^* see Fenton and Griffiths [11]. Under Euler-Bernoulli beam theory [12] the effective modulus of elasticity for all loading conditions can be formulated as:

$$E^* = \left(\int_0^L \omega(v) \cdot E(v)^{-1} \, \mathrm{d}v \right)^{-1} \tag{1}$$

where $(.)^{-1}$ denotes the pointwise reciprocal such that $E(v)^{-1} = \left\{ v_i \in D | \frac{1}{E(v_i)} \right\}$ where $D = [0, L]$ is the domain of the integral. The weighting function $\omega(v)$ satisfies the following property:

$$\int_0^L \omega(v) \, \mathrm{d}v = 1 \tag{2}$$

where the units of the weighting function $\omega(v)$ are given by the reciprocal of the units of the domain D so that Equation 2 is dimensionless. The weighting function is dependent on the loading and boundary conditions of the beam and consequently a separate weighting functions for the case of tension $\omega_T(v)$, 3-point $\omega_3(v)$ and 4-point bending $\omega_4(v)$ are presented. It should be noted that this paper does not suggest an equivalence between the profiles of tensile and bending modulus of elasticity but rather the intention of this work is to assess the influence of the midpoint approximation for different loading scenarios. In the case of tension every point in the domain has a equal contribution to the tensile effective modulus of elasticity E_T^* since the stress distribution is spatially constant and consequently E_T^*

is given by an unweighted harmonic mean [11] and consequently every point in the domain D has an equal weighting. The weighting function $\omega_T(v)$ of the tensile effective elastic modulus E_T^* determined from total displacement U_T is given by:

$$\omega_T(v) = \frac{1}{L} \quad \text{if } 0 \leq v \leq L \tag{3}$$

The weighting function $\omega_3(v)$ for the 3-point effective elastic modulus E_3^* determined from midspan deflection U_B is given by [10]:

$$\omega_3(v) = \begin{cases} \dfrac{12v^2}{L^3} & \text{if } 0 \leq v \leq \dfrac{L}{2} \\ \dfrac{12(L-v)^2}{L^3} & \text{if } \dfrac{L}{2} \leq v \leq L \end{cases} \tag{4}$$

The weighting function $\omega_4(v)$ for the 4-point effective elastic modulus E_4^* determined from midspan deflection U_B is given by (derivation in Appendix):

$$\omega_4(v) = \begin{cases} \dfrac{324v^2}{23L^3} & \text{if } 0 \leq v \leq \dfrac{L}{3} \\ \dfrac{108v}{23L^2} & \text{if } \dfrac{L}{3} \leq v \leq \dfrac{L}{2} \\ \dfrac{108(L-v)}{23L^2} & \text{if } \dfrac{L}{2} \leq v \leq \dfrac{2L}{3} \\ \dfrac{324(L-v)^2}{23L^3} & \text{if } \dfrac{2L}{3} \leq v \leq L \end{cases} \tag{5}$$

A comparison of the three weighting functions is shown in Figure 3 for a beam of length $L = 1$ m. It is observed that the 3-point weighting function $\omega_3(v)$ assigns the highest weighting to the centroid of the sample volume $v_c = 0.5$ m followed by the four-point weighting function $\omega_4(v)$ whilst the tensile weighting function $\omega_T(v)$ assigns the lowest centroidal weighting. The 4-point weighting function $\omega_4(v)$ is more uniform over the domain than the 3-point weighting function $\omega_3(v)$ and this is attributed to the constant central bending moment induced by four-point bending (see Equation 27). The derivative of the tension weighting function $\omega_T'(v)$ is continuous over the domain of integration whilst the derivatives of the bending weighting functions, $\omega_3'(v)$ and $\omega_4'(v)$, are discontinuous at the points where deflection is observed and load is applied. It is observed that as the weighting function $\omega(v)$ approaches the Dirac-delta function $\delta(v - v_c)$ [13] then the effective property E^* becomes a point sample of the random field at the centroid v_c and consequently it is expected that the parameter estimates obtained from E_3^* will be the most accurate whilst the parameter estimates obtained from E_T^* will be the least accurate.

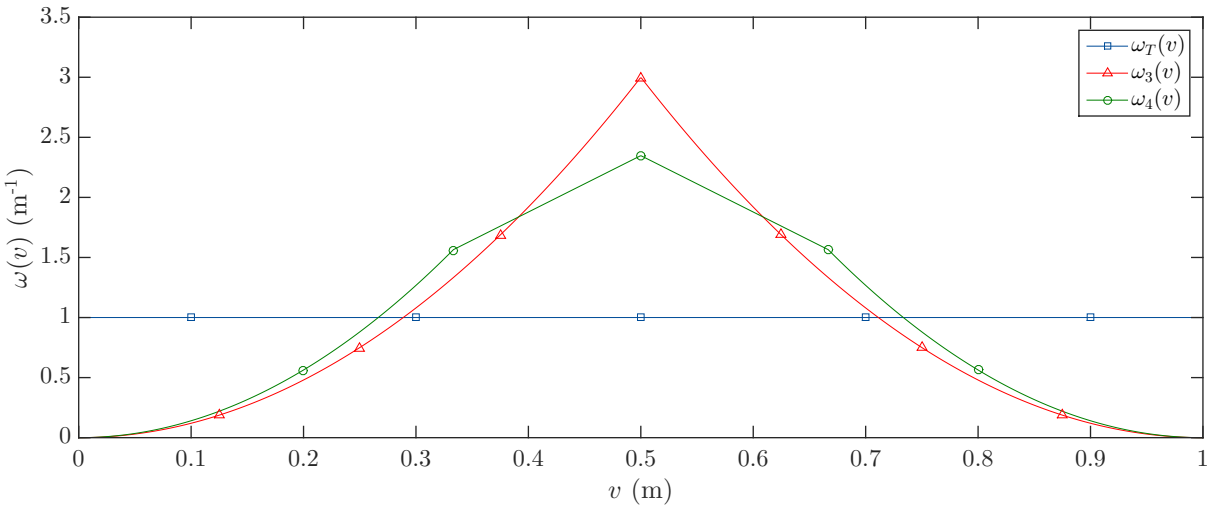

Figure 3: Weighting functions for tensile $\omega_T(v)$, 3-point $\omega_T(v)$ and 4-point $\omega_4(v)$ loading conditions ($L = 1$ m).

2 Computer experiment

A number of researchers have conducted physical experiments into the variation of elastic modulus of timber for the case of tensile loading [14] as well as 3-point [15] and 4-point [16] bending. A computer experiment has been designed to replicate these experiments and quantify the uncertainty associated with estimating the parameters of the random field model directly from the measured effective properties. The experimental procedure involves making $N = 7$ observations of the effective elastic modulus E^* over an effective length of $L \approx 0.43$ m on a beam of total length $L_0 = 3$ m for a total of $M = 20$ beams as shown in Figure 4. The effective elastic modulus E^* is no longer a constant but rather a piecewise continuous function notated by $E^*(v)$. The Monte Carlo method is used to replicate the experimental procedure a total of $R = 1 \times 10^6$ times in order to analyse the uncertainty associated with the parameter estimates. In particular the aleatoric and epistemic uncertainty is quantified for the estimate $\hat{\mu}$ of the location parameter μ, the estimate $\hat{\sigma}$ of the scale parameter σ and the estimate $\hat{\theta}$ of the correlation parameter θ.

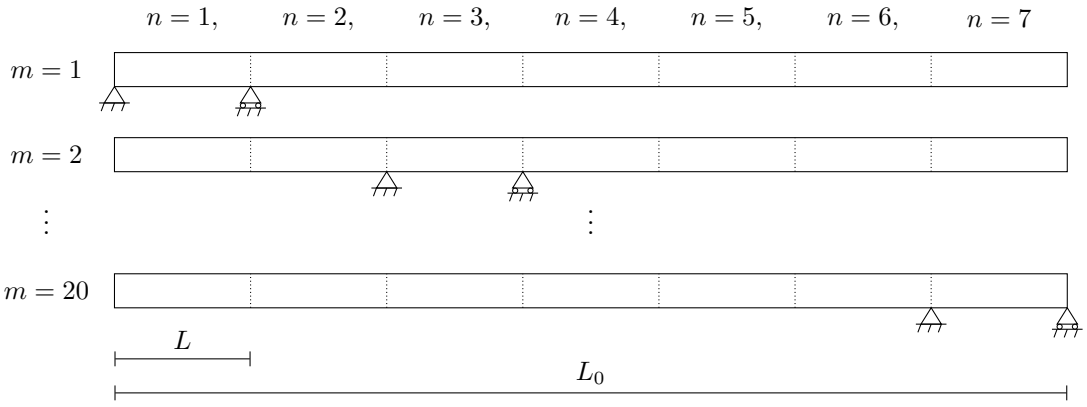

Figure 4: Setup of the computer experiment where effective properties $E^*_{n,m}$ are observed over $N = 7$ segments of length $L \approx 0.43$ m for a total of $M = 20$ beams of length $L_0 = 3$ m.

The experimental procedure requires the generation of synthetic stiffness profiles designed which model spatial variation in stiffness along the beam. Since negative values for elastic modulus are not physically permissible the maginal distribution of $E(v)$ was selected as lognormal since this distribution is strictly non-negative. Thus the stiffness profile is a lognormal stochastic process $E(v)$ with location parameter $\mu = 10$ GPa, scale parameter $\sigma = 3$ GPa and the exponential correlation function [17]:

$$\rho(\tau) = \exp\left(-\frac{2|\tau|}{\theta}\right) \tag{6}$$

where $\tau = |v_1 - v_2|$ is the absolute separation between points in the domain $D = [0, L_0]$ and the value of the correlation length θ is taken to be 0.6 m. The exponential correlation function is selected since it produces realisations which are not smooth which is realistic of material properties [18]. A single realisation of the base random field $E(x)$ is shown in Figure 5 along the 3-point effective elastic moduli $E^*_3(v)$ determined according to the experimental procedure illustrated in Figure 4.

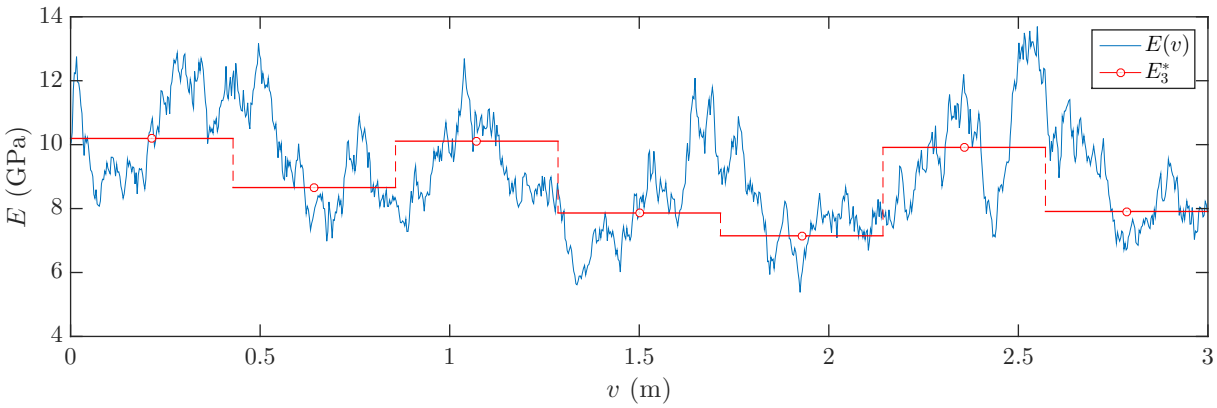

Figure 5: One realisation of the base process $E(v)$ and its piecewise constant profile of 3-point effective elastic modulus E^*_3.

3 Simulation

The approach adopted to simulate the lognormal process $E(v)$ is to first simulate the underlying Gaussian process $E_G(v)$ and then obtain $E(v)$ through:

$$E(v) = \exp\left(E_G(v)\right) \tag{7}$$

Inconveniently the operation of exponentiation alters the statistical moments of $E_G(v)$ and consequently in order to obtain a lognormal process $E(v)$ with specified statistics μ, σ^2, $\rho(\tau)$ the approach is to backconfigure the properties μ_G, σ_G^2, $\rho_G(\tau)$ of the Gaussian process $E_G(v)$ using the following relationships [6]:

$$\mu_G = \ln\left(\mu\left(1+\frac{\sigma^2}{\mu^2}\right)^{-\frac{1}{2}}\right) \tag{8}$$

$$\sigma_G^2 = \ln\left(1+\frac{\sigma^2}{\mu^2}\right) \tag{9}$$

$$\rho_G(\tau) = \frac{\ln\left(\rho(\tau)(\exp(\sigma^2)-1)+1\right)}{\sigma^2} \tag{10}$$

The numerical simulation of the Gaussian process $E_G(v)$ requires that it be discretised and a common method to achieve this also happens be the midpoint approximation. It should be recognised that the midpoint approximation is not only widely used for estimation but also for the simulation of random fields and it is the ubiquitousness of this approximation that motivates this research into the uncertainty associated with it. Under the midpoint approximation $E_G(v)$ is approximated in each element Ω_e with a piecewise constant function $\bar{E}_G(v)$ given by the value of the field at the centroid v_c of the element:

$$\bar{E}_G(v) = E_G(v_c),\ v \in \Omega_e \tag{11}$$

The discretised field $\bar{E}_G(v)$ is then given by a random vector $\boldsymbol{E_G} = \{E_G(v_c^1), \ldots, E_G(v_c^K)\}$ where $K = 1050$ is the number of elements. Since $E_G(v)$ is a Gaussian random field then $\boldsymbol{E_G}$ is multivariate normal random vector with mean μ_G, standard deviation σ_G and correlation matrix $\boldsymbol{\Sigma_G}$. The method adopted to simulate the Gaussian random vector $\boldsymbol{E_G}$ is covariance matrix decomposition [19] which is based on the follow decomposition of $\boldsymbol{E_G}$:

$$\boldsymbol{E_G} = \mu_G + \sigma_G \boldsymbol{\psi}\boldsymbol{\xi} \tag{12}$$

where μ_G and σ_G are the mean and standard deviation of the underlying normal random field $E_G(v)$, $\boldsymbol{\xi}$ is a column vector of K uncorrelated mean-zero, unit variance normal random variables and $\boldsymbol{\psi}$ is a K by K matrix that satisfies the following decomposition of the correlation matrix $\boldsymbol{\Sigma_G}$:

$$\boldsymbol{\psi}\boldsymbol{\psi}^T = \boldsymbol{\Sigma_G} \tag{13}$$

where $\boldsymbol{\psi}$ is obtained as a lower-triangular matrix through Cholesky decomposition [20]. The discretised approximation to $E(v)$ is then obtained through $\boldsymbol{E} = \exp(\boldsymbol{E_G})$. Note that since $E_G(v)$ was discretised according to the midpoint approximation method then $E(v)$ is also similarly discretised. In each segment the random field is discretised into $K^* = 150$ elements and the effective property of the n^{th} segment of the m^{th} beam $E_{n,m}^*$ is obtained by discretising the integral in Equation 1 for instance the effective property of the first segment of the m^{th} beam is given by:

$$E_{1,m}^* = \frac{K^*}{L\sum_{k=1}^{K^*}\frac{\omega(v_k)}{E_m(v_k)}} \tag{14}$$

4 Estimation

Estimates of the location μ and scale σ parameter of the random field model can be obtained from the observed effective properties $E_{n,m}^*$ using the following method of moments estimators:

$$\hat{\mu} = \frac{1}{NM}\sum_{m=1}^{M}\sum_{n=1}^{N} E_{n,m}^* \tag{15}$$

$$\hat{\sigma}^2 = \frac{1}{NM-1} \sum_{m=1}^{M} \sum_{n=1}^{N} \left(E^*_{n,m} - \hat{\mu}\right)^2 \tag{16}$$

where N is the number of segments over which E^* is observed and M is the number of beams. These estimators are simply the sample mean and variance and are optimal for the case that the samples are statistically independent however since the effective properties are correlated along the length of the beam this is another source of epistemic bias that is quantified in the Section 5.

A common approach to estimate the correlation parameter θ is to compute the sample correlation function also known as the correlogram [21] and then use regression to estimate the value of θ that minimises the misfit between the sample correlation function $\hat{\rho}(\tau)$ and theoretical model $\rho(\tau)$ [22]. However this procedure is computationally expensive for the number of simulations $R = 1 \times 10^6$ required by the computer experiment and consequently a computationally simpler approach is pursued here. Instead of considering the full autocorrelation structure only the lag-1 correlation between adjacent effective properties is considered. An estimator of the lag-1 correlation coefficient ρ_1 is given by:

$$\hat{\rho}_1 = \frac{1}{M(N-1)\,\hat{\sigma}} \sum_{m=1}^{M} \sum_{n=1}^{N-1} \left(E^*_{n,m} - \hat{\mu}\right)\left(E^*_{n,m} - \hat{\mu}\right) \tag{17}$$

An estimate of the correlation length of the exponential correlation function is obtained from the lag-1 correlation coefficient $\hat{\rho}_1$ by changing the subject of Equation 6 to θ and substituting the length over which the effective property was observed $\tau = L$:

$$\hat{\theta} = -\frac{2L}{\ln\left(\hat{\rho}_1\right)} \tag{18}$$

where $L \approx 0.43$ m. In the case of high aleatoric uncertainty due to limited sample size a negative value may be obtained for the lag-1 correlation coefficient $\hat{\rho}_1$ in which case the correlation length estimate $\hat{\theta}$ would be complex which is not physically meaningful. The approach utilised to resolve this issue is to set the $\hat{\theta}$ equal to zero in the case that $\hat{\rho}_1$ is estimated as having a negative value.

5 Results

This section presents the results of the computer experiment into the distribution of the parameter estimates $\{\hat{\mu}, \hat{\sigma}, \hat{\theta}\}$ of the random field. The statistics of these estimated parameters are referred to as *meta-statistics* in order to distinguish them from the statistics of the random field. Two non-normalised meta-statistics are considered for each parameter estimate namely the sample mean Mean[.] and variance Var[.]. The deviation of the Mean[.] of the parameter estimates from the true value of the parameters ($\mu = 10$ GPa, $\sigma = 3$ GPa, $\theta = 0.6$ m) is a measure of the uncertainty due to epistemic error. A normalised meta-statistic, percentage bias Bias[.], is introduced to facilitate comparison of the epistemic uncertainty between different parameter estimates:

$$\text{Bias}\left[\hat{\mu}\right] = \frac{100\%}{R} \sum_{r=1}^{R} \left(\frac{\hat{\mu}_r - \mu}{\mu}\right) \tag{19}$$

where R is the number of simulation, $\hat{\mu}_r$ is the parameter estimate associated with the r^{th} simulation and μ is the true value of the parameter. The total bias estimated by the meta-statistic Bias[.] consists of bias due to both the midpoint approximation and the bias associated with the estimators presented in Section 4. The meta-statistics of point estimates from the base process $E(v)$ are also presented since the bias in these estimates is only due to estimator bias and this enables inferences on what proportion of the bias is due to estimator bias in comparison to the midpoint approximation for the estimates obtained from effective properties. The meta-statistic Var[.] quantifies the aleatoric uncertainty in each of the parameter estimates of the random field. This uncertainty is due to a number of factors including the non-ergodicity of each realisation of $E(v)$, the limited number of beams M and sections N over which the effective properties E^* are observed. The normalised meta-statistic maximum absolute percentage error MAPE[.] [23] is utilised to evaluate total uncertainty resulting from both aleatoric and epistemic uncertainty:

$$\text{MAPE}\left(\hat{\mu}\right) = \frac{100\%}{R} \sum_{r=1}^{R} \left|\frac{\hat{\mu}_r - \mu}{\mu}\right| \tag{20}$$

5.1 Distribution of sample mean

Figure 6 presents the distribution of the parameter estimate $\hat{\mu}$ for each of the tests whilst Table 1 details the four meta-statistics obtained for each parameter estimate. The bias in μ for the base process $E(v)$ was found to be negligible despite the sample mean not being an unbiased estimator for correlated samples. All of the effective properties $\{E_T^*,\ E_3^*,\ E_4^*\}$ have decreased expected value compared to the base process $E(v)$ with expected value $\mu = 10$ GPa. This is due to the effective properties being given by a harmonic mean which tends towards the least elements of the set and consequently the effective properties are disproportionately affected by regions of low stiffness. This effect is weaker for bending behaviour because weak-zones near the supports do not significantly affect expected value however in the case of tensile loading the effect of weak-zones on the effective property E^* is independent of spatial position due to the uniform tensile weighting function $\omega_T(v)$. The deviation in the expected value of the location parameter $\hat{\mu}$ is slightly greater for the case of 4-point bending since the weighting function $\omega_4(v)$ is closer to uniform than the 3-point weighting function $\omega_3(v)$.

A similar variance was observed for all the tests suggesting that the aleatoric uncertainty in the location parameter estimate $\hat{\mu}$ is not significantly does not vary significantly between tests. In particular the aleatoric uncertainty is similar for estimates of μ from the base process $E(v)$ and estimates of μ from its effective property E^*. This is due to the fact that the variance of the arithmetic mean of a set of random variables does not deviate significantly from the variance of the harmonic mean of the same set. The variance is slightly greater for 3-point bending and this is explained by considering that as the weighting function $\omega(v)$ approaches the Dirac delta function $\delta(v - v_c)$ the effective property E^* is in effect averaging over an increasingly small statistical region and consequently variance in the estimate increases. MAPE[.] is similar for all tests suggesting that the epistemic uncertainty due to the midpoint approximation is small compared to the aleatroic uncertainty associated with $M = 20$ realisations of the beam stiffness profile $E(v)$ for the experimental setup detailed in Figure 4.

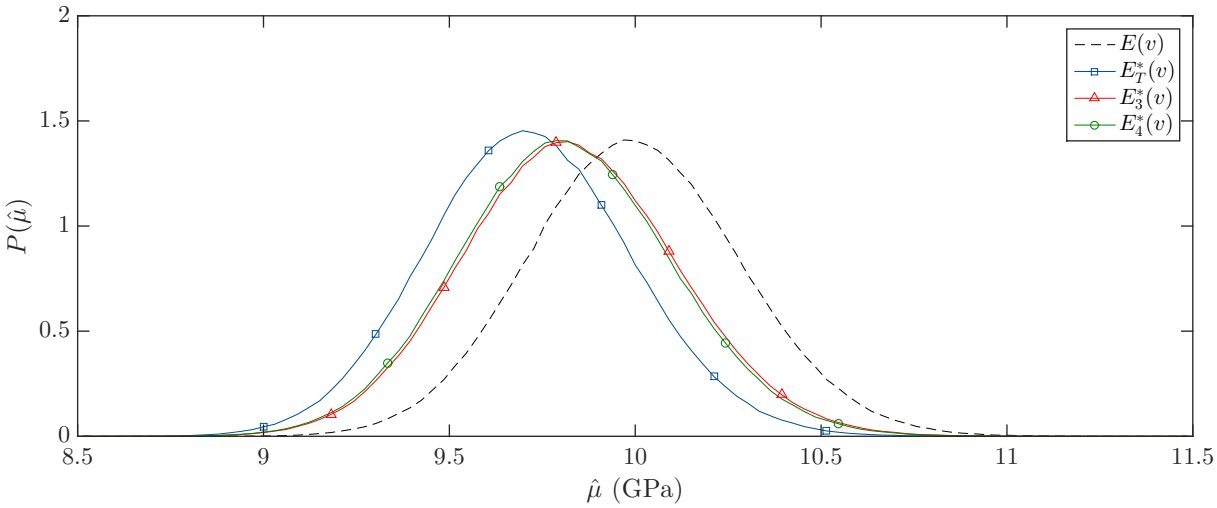

Figure 6: Distribution of location parameter estimate $\hat{\mu}$ for tension $E_T^*(v)$, 3-point $E_3^*(v)$ and 4-point $E_4^*(v)$ bending tests with base distribution $E(v)$ shown for comparison.

Table 1: Meta-statistics of the location parameter estimate $\hat{\mu}$.

Observed process		Mean[$\hat{\mu}$]	Var[$\hat{\mu}$]	Bias[$\hat{\mu}$]	MAPE[$\hat{\mu}$]
name	*symbol*	(GPa)	(MPa^2)	(%)	(%)
Base	$E(v)$	10.00	80.9	0.00	2.27
Tension	$E_T^*(v)$	9.71	76.1	−2.85	3.30
3-point	$E_3^*(v)$	9.83	82.1	−1.75	2.72
4-point	$E_4^*(v)$	9.81	81.3	−1.87	2.76

5.2 Distribution of sample standard deviation

Figure 7 presents the distribution of the scale parameter estimate $\hat{\sigma}$ for each of the tests whilst Table 2 details the four meta-statistics obtained for each parameter estimate. Figure 7 shows that the estimates of the scale parameter $\hat{\sigma}$ obtained from the effective properties $\{E_T^*,\ E_3^*,\ E_4^*\}$ underestimate the true variability of the base process $E(v)$. This underestimation of the true variability of the base process $E(v)$ is unconservative since under random field theory the beam would be modelled as being inappropriately homogeneous. The trends are similar to those observed for $\hat{\mu}$ and the reduction in the expected value of $\hat{\sigma}$ is once again greatest for tensile loading E_T^* and at a minimum for 3-point bending E_3^*. Table 2 shows that the estimator of standard deviation $\hat{\sigma}$ is negatively biased for the base process $E(v)$ and consequently it is concluded that the estimator of the scale parameter in Equation 16 has a negative bias of approximately 0.66%. Thus approximately 0.66 percentage points of the Bias [.] reported for the effective properties E^* is attributable to estimator bias and not the epistemic bias due to the midpoint approximation.

There is not a significant variation between the meta-statistic Var[$\hat{\sigma}$] for each effective property and consequently it is concluded that estimating the location and scale parameters of the base process from its effective properties does not siginificantly increase the aleatoric uncertainty associated with estimates of either the location μ or scale parameter σ. The MAPE[.] meta-statistic suggests that for $\hat{\sigma}$ the epistemic uncertainty is significantly greater than the aleatoric uncertainty whilst for $\hat{\mu}$ they are of similar magnitude. Both of the parameter estimates $\hat{\mu}$ and $\hat{\sigma}$ experience a reduction in expected value when estimated from the effective properties however it should be noted that whilst underestimation of μ is conservative the underestimation of σ is not and consequently there is a necessity to develop appropriate methodologies to correct for the epistemic error in the scale parameter estimate $\hat{\sigma}$ so that the stochastic finite element model appropriately quantifies the risk associated with heterogeneous structures.

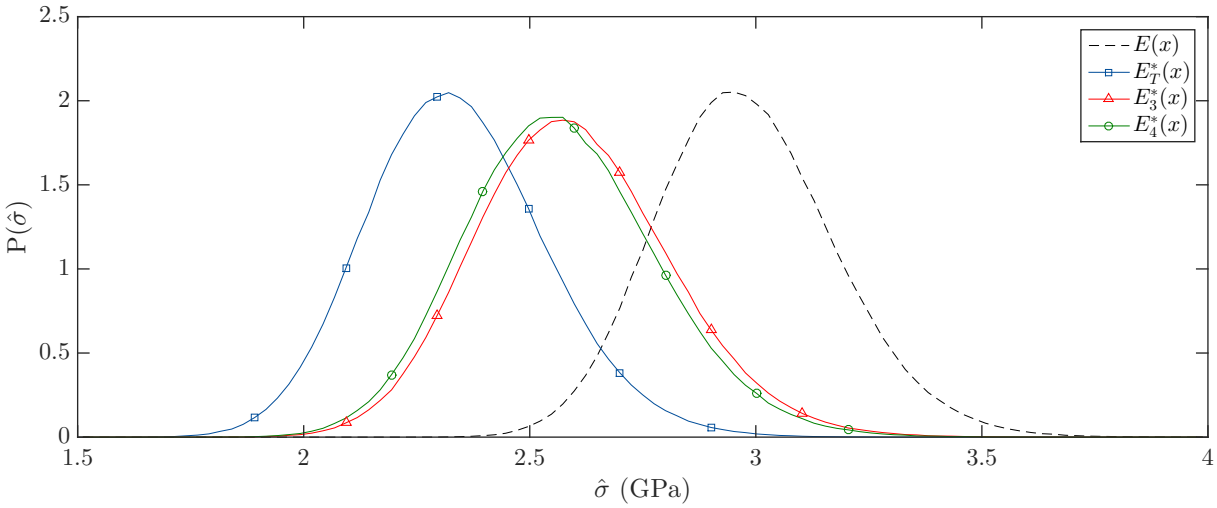

Figure 7: Distribution of scale parameter estimate $\hat{\sigma}$ for tension $E_T^*(v)$, 3-point $E_3^*(v)$ and 4-point $E_4^*(v)$ bending tests with base distribution $E(v)$ shown for comparison.

Table 2: Meta-statistics of the scale parameter estimate $\hat{\sigma}$.

Observed process		Mean[$\hat{\mu}$]	Var[$\hat{\mu}$]	Bias[$\hat{\mu}$]	MAPE[$\hat{\mu}$]
name	*symbol*	(GPa)	(MPa^2)	(%)	(%)
Base	$E(v)$	2.98	38.8	−0.7	5.3
Tension	$E_T^*(v)$	2.34	39.1	−22.0	22.0
3-point	$E_3^*(v)$	2.60	46.2	−13.4	13.7
4-point	$E_4^*(v)$	2.57	45.3	−14.3	14.5

5.3 Distribution of correlation length

Figure 8 presents the distribution of the parameter estimate $\hat{\theta}$ for each of the tests whilst Table 3 details the four meta-statistics of $\hat{\theta}$ for each test. Figure 8 shows that all of the parameter estimates $\hat{\theta}$ obtained from the effective properties $\{E_T^*,\ E_3^*,\ E_4^*\}$ exhibit large positive biases in comparison to the negative

biases observed for both $\hat{\mu}$ and $\hat{\sigma}$. This is due to the effective properties acting to average and therefore smooth the base process $E(v)$ thus greatly increasing measured correlation. The Bias[.] in $\hat{\theta}$ for the base process $E(v)$ in Table 3 indicates that the lag-1 correlation length estimator given by Equation 18 has a negative bias of approximately 1%. The small magnitude of this underestimation indicates the lag-1 estimator is a good estimator of the correlation length θ provided the number of samples is sufficiently large. However this negative bias implies that the true increase in correlation caused by estimating from the effective properties is greater than that suggested by the Bias[.] meta-statistic in Table 3 by approximately a single percentage point.

The uncertainty associated with estimating θ from effective properties is significantly higher than estimating θ directly from the base process $E(v)$. This is unsurprising since the estimator of lag-1 correlation given by Equation 18 depends on both $\hat{\mu}$ and $\hat{\sigma}$ and consequently the uncertainty associated with both of these parameter estimates is propagated into the estimate of the correlation length θ. Estimating from the effective properties E^* did not lead to a significant increase in aleatroic uncertainty for $\hat{\mu}$ and $\hat{\sigma}$ however the aleatroic uncertainty is significantly increased for $\hat{\theta}$ and this is due to the significant distortion of the correlation information caused by the weighted harmonic mean in comparison to the distortion observed for either location or scale information. The MAPE[.] meta-statistic shows that both the aleatoric and epistemic uncertainties have a similar contribution to total uncertainty however it is not possible to make a general conclusion as to whether the overestimation of the correlation length is conservative or unconservative.

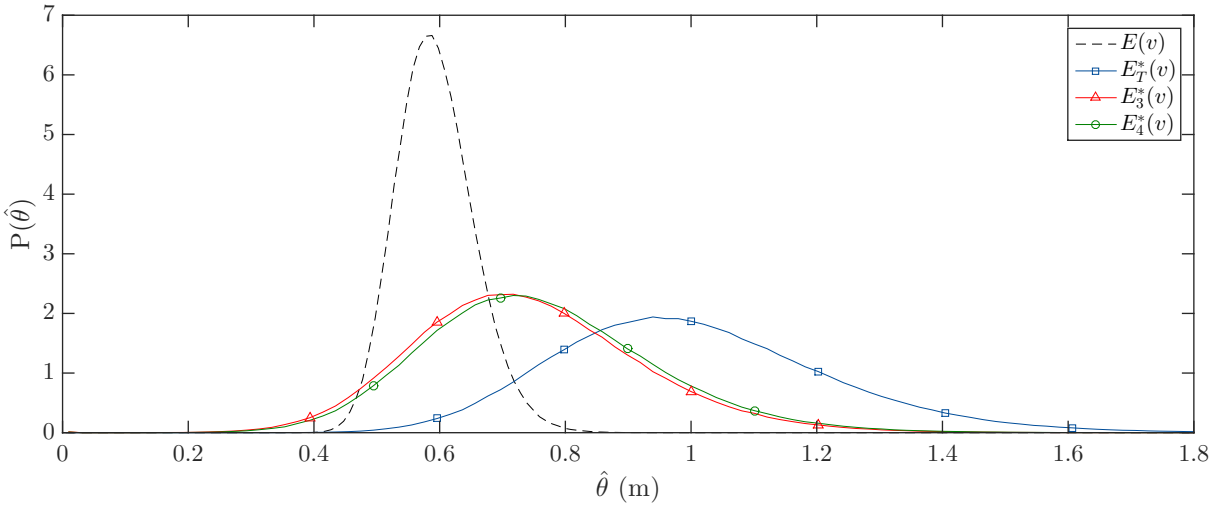

Figure 8: Distribution of correlation parameter estimate $\hat{\theta}$ for tension $E_T^*(v)$, 3-point $E_3^*(v)$ and 4-point $E_4^*(v)$ bending tests with base distribution $E(v)$ shown for comparison

Table 3: Meta-statistics of the correlation parameter estimate $\hat{\theta}$.

Observed process		Mean[$\hat{\mu}$]	Var[$\hat{\mu}$]	Bias[$\hat{\mu}$]	MAPE[$\hat{\mu}$]
name	*symbol*	(GPa)	(MPa^2)	(%)	(%)
Base	$E(v)$	0.59	3.8	−1.1	8.2
Tension	$E_T^*(v)$	1.00	47.8	+67.5	67.7
3-point	$E_3^*(v)$	0.74	32.7	+23.7	29.9
4-point	$E_4^*(v)$	0.76	33.5	+26.5	31.7

6 Conclusion

The computer experiment has shown that estimating random field parameters from the effective properties $\{E_T^*, E_3^*, E_4^*\}$ using the midpoint approximation results in a minor negative epistemic bias in the location parameter $\hat{\mu}$, a moderate negative epistemic bias in the scale parameter $\hat{\sigma}$ and a large positive epistemic bias in the correlation parameter $\hat{\theta}$. The aleatoric uncertainty associated with estimates of μ and σ obtained from effective properties was similar to base aleatoric uncertainty whilst the aleatoric uncertainty associated with the estimate of θ from the effective properties was significantly greater than base aleatoric uncertainty. The computer experiment was only run for one set of random field parameters ($\mu = 12$ GPa,

$\sigma = 3$ GPa, $\theta = 0.6$ m) however the trends are expected to hold for different parameter values with the magnitude of the trend increasing as either the scale parameter σ increases of the correlation ratio θ/L decreases since this increases the heterogeneity of the beam.

The trends in the meta-statistics of the parameter estimates were consistent for all three tests (tension E_T^*, 3-point E_3^* and 4-point E_4^* bending) however the magnitude of the trend was always greatest for the tension test and smallest for three-point bending. It is concluded that the midpoint approximation is least appropriate for tension due to the uniformity of its weighting function $\omega_T(v)$ and most appropriate for 3-point bending due to the central concentration of its weighting function $\omega_3(v)$. The error induced by the midpoint approximation is lower for the 3-point bending test than the 4-point bending test however this increased accuracy has been found to be insignificant compared to the magnitude of the epistemic error induced by midpoint approximation. It is the recommendation of this paper that further research should focus on the development of a methodology to correct the epistemic biases in the parameter estimates obtained from effective properties. There has been some research conducted on this topic however it has been under the assumption that the effective properties of a beam is an unweighted arithmetic mean [24] which neither accounts for the disproportionate contribution of zones of low stiffness to effective modulus of elasticity or the spatial weighting associated with bending tests.

Acknowledgments

The authors would like to acknowledge the support of both the Resilience Engineering Research Group and the Faculty of Engineering, University of Nottingham in conducting this research.

Appendix

This appendix contains the derivation of the weighting function $\omega_4(v)$ for the effective property E_4^* associated with midspan deflection U_B of a simply supported beam under 4-point loading P_4 as shown in Figure 2. The variables u and v describe spatial variation in the internal bending moment M, elastic modulus E and spatial weighting ω whilst the variable x describes variation in displacement U. Under Euler-Bernoulli beam theory the relationship between beam deflection $U(x)$ and modulus of elasticity $E(v)$ is given by:

$$\frac{\mathrm{d}^2U(x)}{\mathrm{d}x^2} = -\frac{M(v)}{E(v)I} \tag{21}$$

where I is the area moment of inertia which is assumed to be constant. Under the standard theory of double integration beam deflection $U(x)$ is given by:

$$U(x) = \frac{1}{I}\int_0^x \int_0^u \frac{M(v)}{E(v)}\,\mathrm{d}v\,\mathrm{d}u + Cx + D \tag{22}$$

where C and D are the first and second constants of integration respectively. Applying boundary conditions for a simply supported beam, namely that $U(x=0) = 0$ and $U(x=L) = 0$, gives:

$$U(x) = \frac{1}{I}\int_0^x \int_0^u \frac{M(v)}{E(v)}\,\mathrm{d}v\,\mathrm{d}u - \frac{x}{LI}\int_0^L \int_0^u \frac{M(v)}{E(v)}\,\mathrm{d}v\,\mathrm{d}u \tag{23}$$

Through an interchange in the order of integration the double integral can be reduced to a single integral:

$$U(x) = \frac{1}{I}\int_0^x \frac{M(v)}{E(v)}\int_v^x \mathrm{d}u\,\mathrm{d}v - \frac{x}{LI}\int_0^L \frac{M(v)}{E(v)}\int_v^L \mathrm{d}u\,\mathrm{d}v \tag{24}$$

$$= \frac{1}{I}\int_0^x \frac{M(v)(x-v)}{E(v)}\,\mathrm{d}v - \frac{x}{LI}\int_0^L \frac{M(v)(L-v)}{E(v)}\,\mathrm{d}v \tag{25}$$

An expression for midspan deflection U_B is obtained by substituting $x = L/2$ into Equation 24:

$$U_B = \frac{1}{I}\int_0^{L/2} \frac{M(v)(L/2-v)}{E(v)}\,\mathrm{d}v - \frac{1}{2I}\int_0^L \frac{M(v)(L-v)}{E(v)}\,\mathrm{d}v \tag{26}$$

The internal bending moment $M_4(v)$ for four-point loading as shown in Figure 2 is given by:

$$M_4(v) = \begin{cases} -\dfrac{Pv}{2} & \text{if } 0 \le v \le \dfrac{L}{3} \\ -\dfrac{PL}{6} & \text{if } \dfrac{L}{3} \le v \le \dfrac{2L}{3} \\ -\dfrac{P(L-v)}{2} & \text{if } \dfrac{2L}{3} \le v \le L \end{cases} \tag{27}$$

Substituting the equation for expression for bending moment $M_4(v)$ into Equation 26 yields:

$$\begin{aligned} U_B = \frac{P}{I}\Bigg[&- \int_0^{L/3} \frac{2v(L/2-v)}{4E(v)}\,\mathrm{d}v - \int_{L/3}^{L/2} \frac{2L(L/2-v)}{12E(v)}\,\mathrm{d}v \\ &+ \int_0^{L/3} \frac{v(L-v)}{4E(v)}\,\mathrm{d}v + \int_{L/3}^{2L/3} \frac{L(L-v)}{12E(v)}\,\mathrm{d}v + \int_{2L/3}^{L} \frac{(L-v)^2}{4E(v)}\,\mathrm{d}v \Bigg] \end{aligned} \tag{28}$$

Combining terms over similar domains of integration and simplifying gives:

$$\begin{aligned} U_B = \frac{P}{I}\Bigg[&\int_0^{L/3} \frac{v^2}{4E(v)}\,\mathrm{d}v + \int_{L/3}^{L/2} \frac{Lv}{12E(v)}\,\mathrm{d}v \\ &+ \int_{L/2}^{2L/3} \frac{L(L-v)}{12E(v)}\,\mathrm{d}v + \int_{2L/3}^{L} \frac{(L-v)^2}{4E(v)}\,\mathrm{d}v \Bigg] \end{aligned} \tag{29}$$

Under the assumption that the beam is homogeneous with constant modulus of elasticity E_4^* the midspan displacement is given by:

$$U_B = \frac{23L^3P}{648IE_4^*} \tag{30}$$

An equation for the effective property E_4^* is obtained in terms of midspan displacement U_B by changing the subject of Equation 30:

$$E_4^* = \frac{23L^3P}{648IU_B} \tag{31}$$

Substituting the heterogeneous result given by Equation 29 into the homogeneous result given by Equation 31 yields:

$$E_4^* = \frac{23L^3}{648\left(\displaystyle\int_0^{L/3} \frac{v^2}{4E(v)}\,\mathrm{d}v + \int_{L/3}^{L/2} \frac{Lv}{12E(v)}\,\mathrm{d}v + \int_{L/2}^{2L/3} \frac{L(L-v)}{12E(v)}\,\mathrm{d}v + \int_{2L/3}^{L} \frac{(L-v)^2}{4E(v)}\,\mathrm{d}v\right)} \tag{32}$$

The effective property E_4^* for four-point bending is then expressed as a weighted harmonic mean:

$$E_4^* = \left(\int_0^L \omega_4(v) \cdot E(v)^{-1}\,\mathrm{d}v\right)^{-1} \tag{33}$$

where the weighting function $\omega_4(v)$ is given by:

$$\omega_4(v) = \begin{cases} \dfrac{324v^2}{23L^3} & \text{if } 0 \le v \le \dfrac{L}{3} \\ \dfrac{108v}{23L^2} & \text{if } \dfrac{L}{3} \le v \le \dfrac{L}{2} \\ \dfrac{108(L-v)}{23L^2} & \text{if } \dfrac{L}{2} \le v \le \dfrac{2L}{3} \\ \dfrac{324(L-v)^2}{23L^3} & \text{if } \dfrac{2L}{3} \le v \le L \end{cases} \tag{34}$$

References

[1] G. Stefanou, The stochastic finite element method: Past, present and future, *Computational Methods in Applied Mechanics and Engineering* **198**, 1031 (2009).

[2] A. F. Moshtaghin, S. Franke, T. Keller, and A. P. Vassilopoulos, Random field-based modeling of size effect on the longitudinal tensile strength of clear timber, *Structural Safety* **58**, 60 (2016).

[3] T. Most and C. Bucher, Probabilistic analysis of concrete cracking using neural networks and random fields, *Probabilistic engineering mechanics* **22**, 219 (2007).

[4] D. M. Ghiocel and R. G. Ghanem, Stochastic finite-element analysis of seismic soil-structure interaction, *Journal of Engineering Mechanics* **128**, 66 (2009).

[5] R. J. Adler and J. E. Taylor, *Random Fields and Geometry* (Springer, 2007).

[6] E. Vanmarcke, *Random fields: Analysis and synthesis (3rd ed.).* (The MIT Press, 1988).

[7] J. J. McCoy, On the calculation of bulk properties of heterogeneous materials, *Quarterly of Applied Mathematics* **37**, 137 (1979).

[8] A. D. Kiureghian and J.-B. Ke, The stochastic finite element method in structural reliability, *Computational Mechanics Publications* **3**, 83 (1988).

[9] A. D. Kiureghian and O. Ditlevsen, Aleatory or epistemic? Does it matter?, *Structural Safety* **31**, 105 (2009).

[10] F. K. Becthel, Beam stiffness as a function of pointwise E with application to machine stress rating, *Symposium on forest products research international–achievements and the future : 22-26 Apr 1985, Pretoria / org. National Timber Research Institute of the South African Council for Scientific and Industrial Research* (1985).

[11] G. A. Fenton and D. V. Griffiths, *Risk Assessment in Geotechnical Engineering* (Wiley, 2008).

[12] E. Carrera, G. Guinta, and M. Petrolo, *Beam structures: Classical and advanced theories* (Wiley, 2011).

[13] P. A. M. Dirac, *The Principles of Quantum Mechanics* (Oxford University Press, 1967).

[14] R. Brandner and G. Schickhofer, Spatial correlation of tensile perpendicular to grain properties in norway spruce timber, *Wood Science and Technology* **48**, 337 (2014).

[15] S. R. Arwade, P. L. Clouston, and R. Winans, Measurement and stochastic computational modeling of the elastic properties of parallel strand lumber, *Journal of Engineering Mechanics* **135**, 897 (2009).

[16] H. S. Sousa, J. M. Branco, and P. B. Lourenço, Prediction of global bending stiffness of timber beams by local sampling data and visual inspection, *European Journal of Wood and Wood Products* **72**, 453 (2014).

[17] C. E. Rasmussen and C. K. I. Williams, *Gaussian Processes for Machine Learning (Adaptive Computation and Machine Learning)* (The MIT Press, 2005).

[18] M. L. Stein, *Interpolation of spatial data: Some theory for Kriging* (Springer, 1999).

[19] E. M. Scheuer and D. S. Stoller, On the generation of normal random vectors, *Technometrics* **4**, 278 (1962).

[20] G. Fenton, Error evaluation of three random field generators, *Journal of Engineering Mechanics* **120**, 2478 (1994).

[21] N. A. C. Cressie, *Statistics for spatial data* (Wiley, 1993).

[22] M. Lloret-Cabot, G. Fenton, and M. Hicks, On the estimation of scale of fluctuation in geostatistics, *Georisk: Assessment and Management of Risk for Engineered Systems and Geohazards* **8**, 129 (2014).

[23] R. J. Hyndman and A. B. Koehler, Another look at measures of forecast accuracy, *International Journal of Forecasting* **22**, 679 (2006).

[24] W. M. Bulleit and R. A. Chapman, Characterization of the correlation structure of lumber strength properties, *Wood Science and Technology* **38**, 285 (2004).